

Pre-concentration of Toxic Metals using Electrospun Amino-functionalized Nylon-6 Nanofibre Sorbent

Godfred Darko^a, Abdullahi Sobola^a, Sheriff Adewuyi^a,
Jonathan Okechukwu Okonkwo^b and Nelson Torto^{a,*}

^aDepartment of Chemistry, Rhodes University, P.O. Box 94, Grahamstown, 6140, South Africa.

^bDepartment of Environmental, Water and Earth Sciences, Tshwane University of Technology,
175 Nelson Mandela Avenue, Arcadia, Pretoria, 0001, South Africa.

Received 27 October 2011, revised 12 December 2011, accepted 15 December 2011.

Submitted by invitation to celebrate 2011 the 'International Year of Chemistry'.

ABSTRACT

This paper presents a new approach for pre-concentrating toxic metals (As, Cd, Ni and Pb) in aqueous environments using an amino-functionalized electrospun nanofibre sorbent. The sorbent, composed of nanofibres of average diameter 80 ± 10 nm and specific surface area of $58 \text{ m}^2 \text{ g}^{-1}$, exhibited fast adsorption kinetics (<20 min) for As, Cd, Ni and Pb. The optimal pH for the uptake of As, Cd, Ni and Pb were 5.5, 6.0, 6.5 and 11, respectively. The adsorption process best fitted the Freundlich isotherm and followed the first-order kinetics. The highest pre-concentration achieved using the sorbent was 41.99 (Ni in treated wastewater). The capacity of the sorbent to pre-concentrate the toxic metals was compared with those of aqua regia and $\text{HNO}_3 + \text{H}_2\text{O}_2$ digestions. The pre-concentration factors achieved for Cd in river water samples can be ranked as aqua regia digestion (0.73) > adsorption (0.34) > $\text{HNO}_3 + \text{H}_2\text{O}_2$ (0.23) digestion. A similar trend was observed for Ni in river water as well as Ni and Cd in tap water samples. Pb ions in the river water samples were pre-concentrated slightly better using the two digestion methods (pre-concentration factors ~ 22) compared to adsorption method (pre-concentration factor ~ 21). The use of the electrospun amino-functionalized nanofibre sorbent presents an efficient and cost-effective alternative for pre-concentration of toxic metals in aqueous environments.

KEYWORDS

Electrospinning, pre-concentration, heavy metals, nylon-6.

1. Introduction

Analyte pre-concentration is a very important sample preparation step in the determination of toxic metals in aqueous samples. This is because the metals occur only at low concentrations (usually $<1 \text{ mg L}^{-1}$) in groundwater samples and could pass through many analytical instruments undetected due to matrix interference.¹ Pre-concentration strategies are therefore needed to enhance the detectability of the metals for their determination. Water samples are routinely digested with acids to release the metals into solution and also to pre-concentrate the metal ions prior to their determination.

Even though the acid digestion protocol is effective in releasing the metal ions into solutions for analysis, it is cumbersome and renders the samples susceptible to cross-contamination mainly due to the multiple steps that samples are taken through.² Also, the acid digestion approach calls for transporting large volumes of contaminated water samples into the laboratory. This increases the cost of analysis and also exposes the laboratory to contamination.

In order to address the drawbacks, methodologies that will allow *in situ* sampling as well as clean-up and analyte pre-concentration are preferred. Among the pre-concentration procedures available, adsorption processes are more promising because they offer advantages such as large pre-concentration factors obtainable in a short time, simplicity of separation and sorbent reusability.³ The suitability of resins,^{4,5} porous materi-

als,^{6,7} bentonite,⁸ alumina,⁹ biomass,^{10–15} sediments,¹⁶ and substituted naphthalene¹⁷ as sorbents for toxic metals in water has also been assessed. Even though most of the sorbents could adsorb toxic metals, they could not adequately desorb the metals back into solutions for quantification. The applications of the aforementioned sorbents were, therefore, limited to mopping or cleaning-up the metals from water and not for preparing the sample for quantification purposes.

Sorbents prepared from electrospun nanofibres have come to the forefront of analyte pre-concentration due to their superior innate characteristics such as high specific surface area, porosity, flexibility for surface functionalization and ability to conform to a wide variety of physical and chemical conditions. Their large surface areas, for example, offer the nanofibres enhanced adsorption capacities.¹⁸ Moreover, the surface of the nanofibres could be functionalized with moieties that have high affinities for metals to increase sensitivity. The metals adsorbed could easily be leached back into solutions, by pH adjustments, to render them available for quantification without affecting the integrity of the sorbent.

Electrospun nanofibres have been functionalized with enzymes and ligands for applications in membrane-based bioreactors^{19–22} or for selective uptake of toxic metals in water. In our laboratory, for instance, a number of polymers have been electrospun and applied as sorbents for adsorbing analytes from matrices.^{23,24} Sorbents derived from electrospun polystyrene and polysulfone functionalized metal-ligands have been tested for their metal

* To whom correspondence should be addressed. E-mail: n.torto@ru.ac.za

adsorbing potentials. Although the sorbents achieved adsorbing capacities higher than those of some of the materials already investigated,^{7,11} their efficiencies declined sharply with increased usage.²⁵ The decline in efficiency was ascribed to the brittle nature of the polymer used. It was said that traces of the sorbent might have flaked off during the adsorption-desorption processes leading to sequential decrease in sorbent mass upon successive usage. If loss of sorbent material was the reason for the decline in efficiency, then chemically coupling the ligand with a mechanically stable polymer such as nylon-6 would be the solution.

In this work, nylon-6 was surface-functionalized with a Schiff base ligand, 2-((Z)-(2-aminophenylimino)methyl)-6-methoxyphenol, prior to electrospinning. The nanofibre membranes were stamped out into disks and were employed as sorbent for uptake of toxic metals from water samples. The capacity of the sorbent to pre-concentrate toxic metals (As, Cd, Ni and Pb) was compared with those of conventional acid digestion protocols.

2. Experimental

2.1. Chemicals and Reagents

Nylon-6 ($M_w = 10\,000$), nitrate salts of Cd(II), Ni(II), and Pb(II) as well as As_2O_3 , all of purity more than 99.0 %, were purchased from Sigma-Aldrich (St. Louis, USA). Formic acid (98 %), glacial acetic acid (99 %), 1,1-carbonyldiimidazole and 1,8-diazabicyclo[5,4]undec-1-ene were purchased from Merck Chemicals, (Wadeville, South Africa). All other chemicals were of analytical grade and were used without any further purification. Standard solutions were freshly prepared using ultrapure water generated from MilliQ systems (Massachusetts, USA). All the glassware was soaked in 10 % HNO_3 for at least 16 h, and then rinsed with double de-ionized water to remove metal contamination. Schiff base ligand, 2-((Z)-(2-aminophenylimino)methyl)-6-methoxyphenol (AMMP) was synthesized through a condensation reaction between an ethanolic solution of 2-hydroxyl-3-methoxybenzaldehyde and 1,2-phenylenediamine (Scheme 1).

2.2. Apparatus and Instruments

2.2.1. Structure Elucidation

Attenuated total reflection infrared spectra ($400\text{--}4000\text{ cm}^{-1}$) were recorded on a Perkin Elmer Spectrum 100 FT-IR spectrometer (Massachusetts, USA), equipped with a universal attenuated total reflection (ATR) sampling accessory. For each spectrum an average of 16 scans with a resolution of 4 cm^{-1} was taken. Each sample was scanned at three different locations. The $^1H\text{-NMR}$ spectrum was recorded in deuterated $CDCl_3$ using $SiMe_4$ as internal standard on BRUKER NMR instrument operating at 400 MHz.

2.2.2. Scanning Electron Microscope Analysis

The morphology of the nanofibres was studied using the

Tescan (TS5 136ML) field emission scanning electron microscope (Brno, Czech Republic) operating at an accelerated voltage of 30 kV after the samples had been gold-coated. The diameters of the nanofibres were evaluated through the distance transform approach using Scandium software.²⁶ The average diameter of the nanofibres were computed from the diameters of >50 nanofibres per sample.

2.2.3. Pore Size Analysis and BET Surface Area

The Brunauer-Emmett-Teller (BET) surface area and pore size of the nanofibres were measured using an Accelerated Surface Area and Porosimetry System, ASAP 2020, from Micromeritics Co. (DuPont, USA). The samples were degassed overnight in vacuum at $105\text{ }^\circ\text{C}$ and specific surface areas were derived from N_2 gas adsorptions-desorption isotherms ($p/p_0 = 0.05\text{--}0.20$).

2.2.4. Metal Ions Analysis

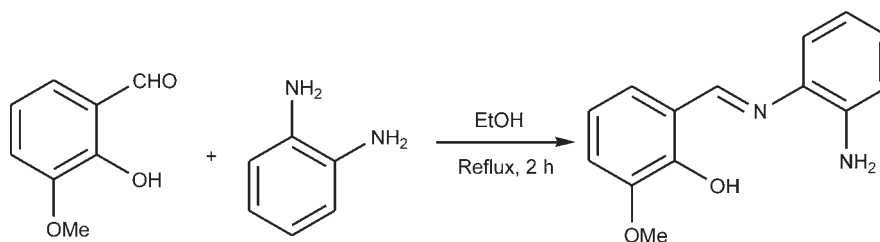
Concentrations of the metals in solutions were measured using Thermo Electron (iCAP 6000 series) Inductively Coupled Plasma-Optical Emission Spectrometer (ICP-OES). Emission lines for the ICP-OES (193.76 nm for As, 226.50 nm for Cd, 231.60 nm for Ni and 220.35 nm for Pb) were selected based on the EPA method of determining trace elements.²⁷ The pH of the solutions was determined using a Jenway (3510) pH meter (Essex, UK).

2.3. Metal Pre-concentration

In order to pre-concentrate toxic metals, the water samples were acid-digested (wet-ashing) using two well-known acid digestion protocols. Otherwise, the metal ions in solution were adsorbed using the sorbent and later desorbed into an acidic solution for quantification. Two acid digestion procedures (using aqua regia or $HNO_3 + H_2O_2$) were separately employed. A 100 mL portion of water sample was pre-digested at room temperature for 16 h using 30 mL aliquot of aqua regia ($HCl + HNO_3$; 3:1) or $HNO_3 + H_2O_2$ (v/v) mixture.²⁸ The suspension was then digested at $130\text{ }^\circ\text{C}$ for 2 h in a reflux condenser. It was then filtered through an ashless Whatman 41 filter, diluted to 100 mL with 0.5 M HNO_3 , and stored in polyethylene bottles at $4\text{ }^\circ\text{C}$ for analyses. Another 100 mL portion of the water sample was spiked with 30 mL of 70 % HNO_3 solution and then filtered through an ashless Whatman 41 filter and stored in polyethylene bottles at $4\text{ }^\circ\text{C}$ for analyses.²⁷ For adsorptions, 20–30 mg portion of the sorbent was placed in 100 mL portion of water sample and stirred intermittently for 2 h. The sorbent was filtered-off and dried using vacuum. The sorbent was then desorbed in 10 mL portion of 0.1 M HNO_3 .

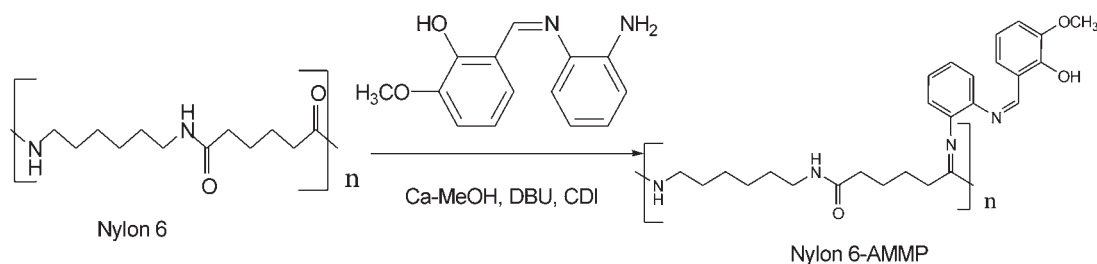
2.4. Metal Adsorption and Desorption Studies

The influence of the initial concentrations of the metal ions was investigated in standard solutions ($0\text{--}10\text{ mg L}^{-1}$). To vials containing 10 mL aliquots of standard solutions 20–30 mg of the sorbent were added and stirred for 2 h. The concentration of metal ions



Scheme 1

Synthesis of 2-((Z)-(2-aminophenylimino)methyl)-6-methoxyphenol, Schiff base ligand.



Scheme 2

Synthesis of functionalized polymer N-(6-(methylamino)hexyl)-6-oxoheptanamide-2-((Z)-(2-aminophenylimino)methyl)-6-methoxyphenol (Nylon-6-AMMP)

left in solution was then determined using ICP-OES after filtering the sorbent. The effect of sorbent dose on the uptake of metals was investigated for masses ranging from 2–30 mg. Portions of the sorbent were placed in 10 mL aliquots of standard solutions and stirred intermittently for 2 h. The sorbent was then filtered off, washed with ultrapure water and was dried on the filter using vacuum suction. The dried sorbent was then placed in 10 mL portion of 0.10 M HNO₃ solution and stirred for 2 min in order to desorb the metals for analysis on ICP-OES. To investigate the optimal pH for metal ions pre-concentration, adsorption experiments were carried out in standard solutions (5 μg L⁻¹) of the metals buffered to the desired pH values ranging from 2 to 12. The extent to which metal ions were enriched was then determined using ICP-OES. The effect of contact time on the uptake of metal ions was also investigated in 5 μg L⁻¹ metal ion solutions in batch experiments. In order to avoid precipitation at higher pH, the solutions were kept at the optimal pH of the metal under study using an ammonia buffer.²⁹

2.5. Functionalization of Nylon-6

Nylon-6 solution was prepared by dissolving 1.5 g (21.5 mmol) in 40 mL Ca-MeOH solvent and refluxing for 2 h at 70 °C.³⁰ After complete dissolution, 1,1-carbonyldiimidazole (0.34 g, 2.1 mmol) and 1.5 mL of 1,8-diazabicyclo[5.4]undec-1-ene in 10 mL of methanol were added to the solution and stirred vigorously for another 30 min. A separately prepared AMMP solution (0.52 g, 2.15 mmol) in 15 mL THF was added drop-wise with continuous stirring for 12 h. On cooling, the solution was slowly poured with vigorous stirring into ethyl ether to precipitate the polymer and was filtered. The obtained polymer mass was washed extensively with ether, acetone and water separately before it was dried overnight *in vacuo* at room temperature.

2.6. Polymer Solution for Electrospinning

For electrospinning, a 12 % solution of the amino-functionalized nylon-6 was prepared in acetic acid/formic acid (1:1) mixture. The polymer mixture was electrospun at a constant flow of 1.0 mL h⁻¹ through a steel needle of 0.8 mm internal diameter onto a collector made of aluminium foil. The needle and the collector were held at optimized voltages of +18 and -5 kV, respectively. Deposition time was kept at 2 h. The formed non-woven nanofibre sorbent was then stamped into circular shape of about 15 mm in diameter corresponding to mass ranging from 20–30 mg.

2.7. Analytical Quality Control Procedure

Two certified reference materials (CRMs) for groundwater were used to validate the analytical procedure; SEP-3, representing high concentrations, and BCR[®]-610, representing low concentrations, were purchased from Inorganic Ventures (Christiansburg, USA) and the Joint Research Centre of the European Commission (Retieseweg, Belgium), respectively.

Analytical calibrations, based on the recommended concentration points and emission lines of each element, were carried out in aqueous standard solutions.²² Adsorption and desorption experiments were carried out using 10 mg of the functionalized nanofibre sorbent in 10 mL portions of the CRMs. Reproducibility of the method was evaluated by comparing the signals obtained from five determinations of the CRMs. The limits of detection (LOD) and quantification (LOQ) were evaluated as 3 and 10 times the estimated regression standard deviation, respectively, based on five replicate determinations.

3. Results and Discussion

3.1. Functionalization and Characterization of Nylon-6

Nylon-6 has a structure in which the N-H groups in the chain are hydrogen bonded to the C=O groups in adjacent chains; thus nylon has good mechanical and chemical stabilities. Consequently, it is difficult to dissolve the polymer before its hydrogen bonds are severed. Although nylon-6 is insoluble in methanol, it was observed to be soluble in hot MeOH/CaCl₂ solution.³⁰ Solubility of nylon in MeOH/CaCl₂ solution was attributed to an initial complex compound formed by calcium with nylon-6, by breaking the hydrogen bonds, thus forcing the polymer into the solvent molecules. Nylon-6 polymer was functionalized by covalently bonding it with AMMP, a multidentate ligand molecule, in a Schiff base condensation reaction (Scheme 2).

A comparison of the FT-IR spectra of the AMMP, nylon-6 and functionalized nylon-6-AMMP polymer (Fig. 1) shows that the changes in the main bond are those anticipated for the covalent functionalization of AMMP with nylon-6. The amide 1 band, which is known to be dominated by the C=O absorption band around 1633 cm⁻¹, is shifted and overlaps with the imine stretching frequency initially at 1618 cm⁻¹ in the AMMP. This spectral change in nylon-6-AMMP polymer is ascribed to interaction of the C=O bond of nylon-6 with the NH₂ group of the AMMP. Also, the sharp N-H bands in nylon-6 and AMMP (3296 and 3362 cm⁻¹, respectively) and AMMP-OH band appeared as broad peak in the new nylon-6-AMMP, suggesting hydrogen bond interaction. In addition, both the symmetrical and asymmetrical -CH₂ stretching modes of nylon-6 around 2870 and 2930 cm⁻¹, respectively, are present in the new nylon-6-AMMP spectrum. The use of ATR is more appropriate in this work because it only scans the surface (up to the depth of 5 μ) of the nanofibre membrane.³¹ The functional groups identified on the spectra can, therefore, be said to be on the surface of the membrane.

3.2. Electrospinning of Functionalized Nylon-6

The morphologies of nanofibres and their formation during electrospinning are dependent on the properties of the polymer solution used.³² Nylon-6 dissolves in formic acid, but not in acetic acid. However, steady states could not be achieved when pure formic acid was used to electrospin nylon-6.³³ Therefore, formic

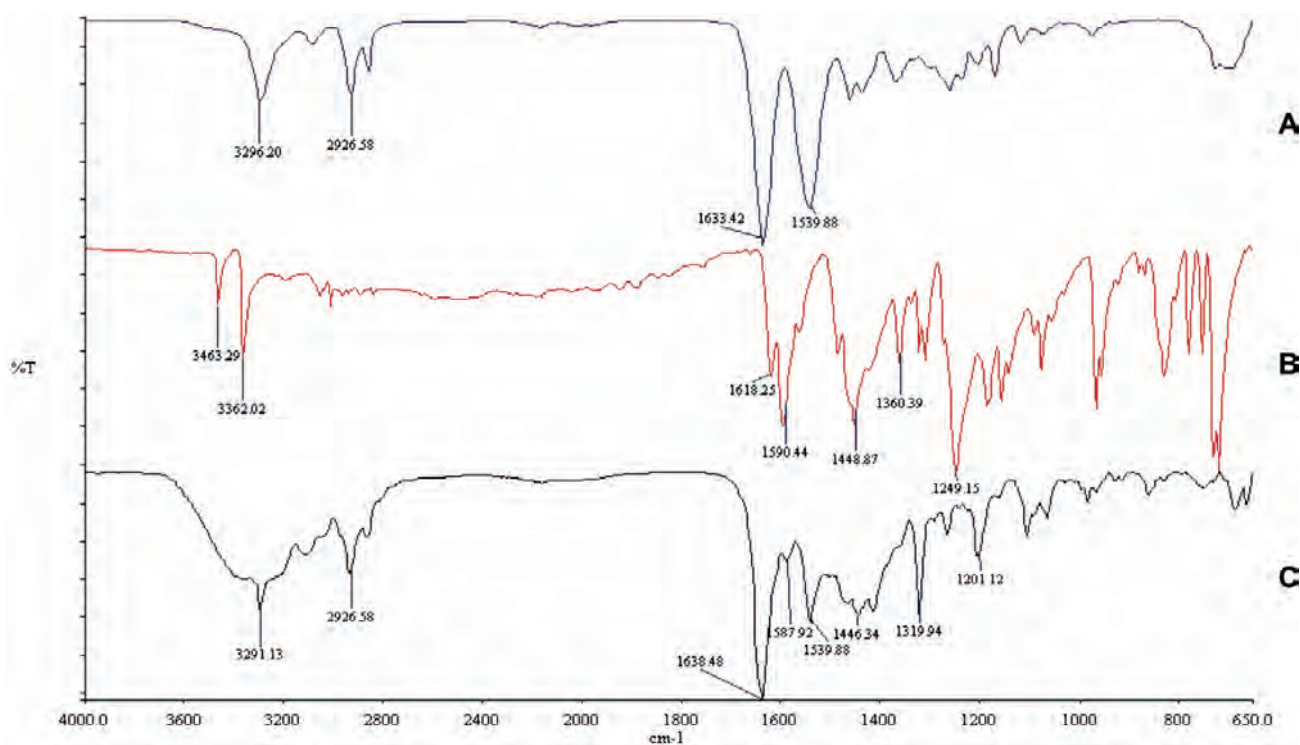


Figure 1 FT-IR spectra of AMMP (A), nylon-6 (B) and functionalized nylon-6-AMMP (C) electrospun nanofibre.

acid was blended with acetic acid in order to achieve steady states during the electrospinning of the functionalized nylon-6. Smooth, non-beaded nanofibres of diameter ranging from 80 nm to 95 nm were obtained (Fig. 2).

3.3. Porosity Measurements

The highly porous nature of nanofibre non-woven produced *via* electrospinning is a key element in their application in many fields.^{34,35} For example, the pore sizes of the sorbent material will control the accessibility of the ligand to the metal ions. The specific surface area of the sorbent defines its efficiency of adsorption. Table 1 shows the pore characteristics of the amino-functionalized nylon-6 sorbent.

The specific surface area of the sorbent is determined by the size of the nanofibres that it is composed of. Nanofibres of smaller diameters produce sorbents of higher surface areas. The average fibre diameter (80 ± 19 nm) and specific surface area (58.10 ± 2.25 m² g⁻¹) generated from electrospinning 12 % nylon-6 in this work, compares favourably with the average diameter of 90 nm and specific surface area of 33 m² g⁻¹ recorded on electrospinning 15 % nylon-6.³⁶ Diameter of electrospun nanofibres are directly proportional to the polymer concentration used. Therefore, 15 %wt concentration was expected to give nanofibres of bigger diameters (smaller specific surface areas) than those from 12 %wt concentration.

Table 1 Pore characteristics of electrospun nylon-6-AMMP nanofibre sorbent.

| Porosity parameter | Measurement |
|--|------------------|
| Average fibre diameter (nm) | 80 ± 19 |
| Specific surface area (m ² g ⁻¹) | 58.10 ± 2.25 |
| Average pore size [§] (Å) | 122 ± 1.61 |
| Micropore volume [‡] (cm ³ g ⁻¹) | 0.08 ± 0.01 |

[§]Specific surface area was calculated using the BET method.

[‡]Average pore size and micropore volume was calculated using the BJH method.

3.4. pH Dependence

The concentration of H⁺ ions in the solution containing the adsorbate is an important criterion in adsorption studies because H⁺ ions compete with the metal cations for the binding sites on the sorbent. The concentration of H⁺ ion in an acidic solution is relatively high and they tend to fill up the binding sites on the sorbent's surface. The H⁺ ions also create a repulsive electrostatic force for the on-coming cations. Adsorption is therefore low in highly acidic solutions (pH less than 4). Adsorption of metals is, however, favoured in less acidic solutions because such solutions contain few competing H⁺ ions and consequently, electrostatic repulsions are low.

The adsorption of the metal ions increased rapidly with the increase in the solution pH until it reached equilibrium where no significant observed change with pH. These adsorption patterns are typical of cations.³⁷ The optimal pH for adsorption was found to be 5.5, 6.0, 6.5 and 11 for As, Cd, Ni and Pb, respectively. No significant adsorptions were observed when the solution pH was less than 3 in all metals studied. This was the expected trend due to high competition between the H⁺ and the metal cations in acidic solutions. The adsorption curves and the optimal pH values obtained in the work are similar to those observed in the previous studies. For example, Ezoddin and co-workers found the pH range of 7–8 as the optimal for quantitative recovery (>95 %) of Cd and Pb on a modified nano- γ -alumina.⁹ Zhou and co-workers observed that no appreciable uptake of metals occurred on thiourea-modified magnetic chitosan microspheres when the solution pH was less than 2.⁴¹ Because the pH of groundwater is often in the range of 5.5–8.5,³⁸ there would be no need for pH adjustments when the sorbent is used in natural water samples. This is of significant importance in applying the sorbent in natural water environments.

3.5. Adsorption Kinetics

Figure 3 shows the adsorption profile of metals with respect to time. The process showed considerably fast kinetics at the initial

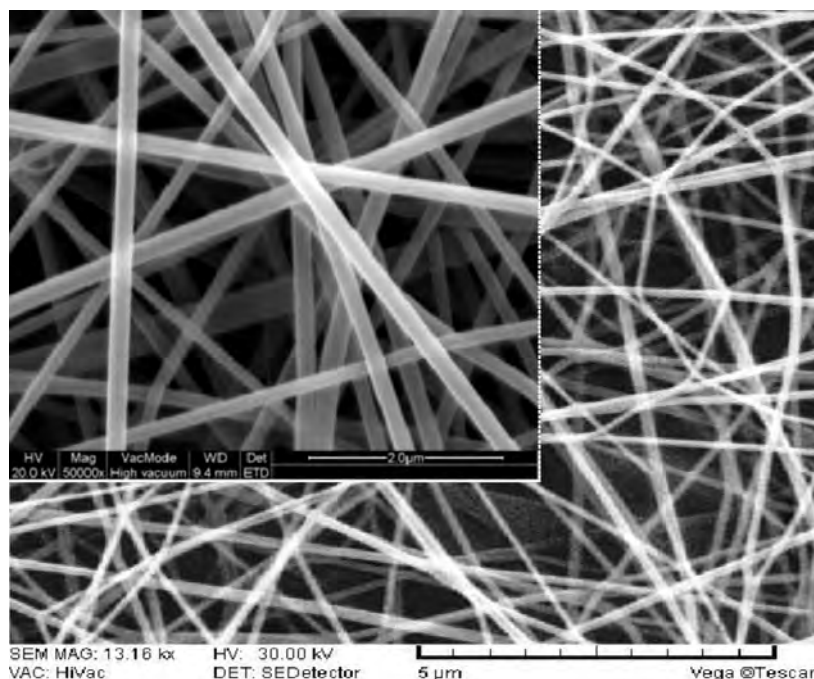


Figure 2 Scanning electron microscopy image of nylon-6-AMMP nanofibres.

period until equilibrium was attained. For example, by the end of the 10th min after application of the sorbent, 97 % of As, 98 % of Cd, 96 % of Ni and 95 % of Pb had already been adsorbed. These equilibration times were shorter than the 3 h recorded for functionalized chitosan sorbents,³⁹ 6 h for an ion imprinted composite⁴⁰ and 8 h for thiourea-modified magnetic chitosan microspheres.⁴¹ According to Pierce and Moore, adsorption processes that are purely due to electrostatic attractions are usually very rapid.⁴² Hence, the results obtained in this work might indicate a hydrogen bond formation between the metal species and the sorbent. Such fast adsorption kinetics is an added advantage of the sorbent as it allows for a high throughput of samples prior to analysis.

3.6. Kinetic Models

Adsorption data obtained were fitted into kinetic models and

first-order kinetics found to best described the process. For first-order reactions, the initial concentration of adsorbate (α) relates to the equilibrium concentration (x) and time (t) as:

$$\ln(\alpha - x) = -kt + \ln \alpha, \quad (1)$$

where k is the rate constant (min^{-1}).

A plot of $\ln(\alpha - x)$ vs t (min) will, therefore, yield a straight line if first-order kinetics is obeyed. Figure 4 shows the first-order kinetics for As, Cd, Ni and Pb while Table 2 shows their correlation coefficients and the rate constants, k .

3.7. Adsorption Isotherms

Adsorption data obtained from standard solutions (concentration range of $1.0\text{--}10 \text{ mg L}^{-1}$) at 25°C were evaluated into known adsorption models and the data best fitted into the Freundlich model. The Freundlich isotherm relates the equilibrium concen-

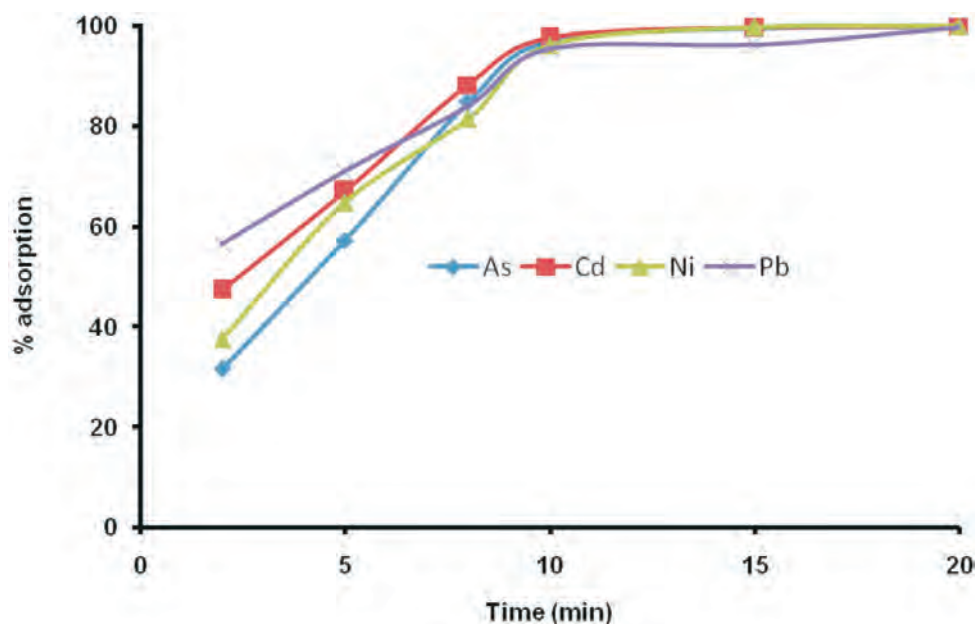


Figure 3 Adsorption kinetics of As, Cd, Ni and Pb on nylon-6-AMMP electrospun nanofibre sorbent.

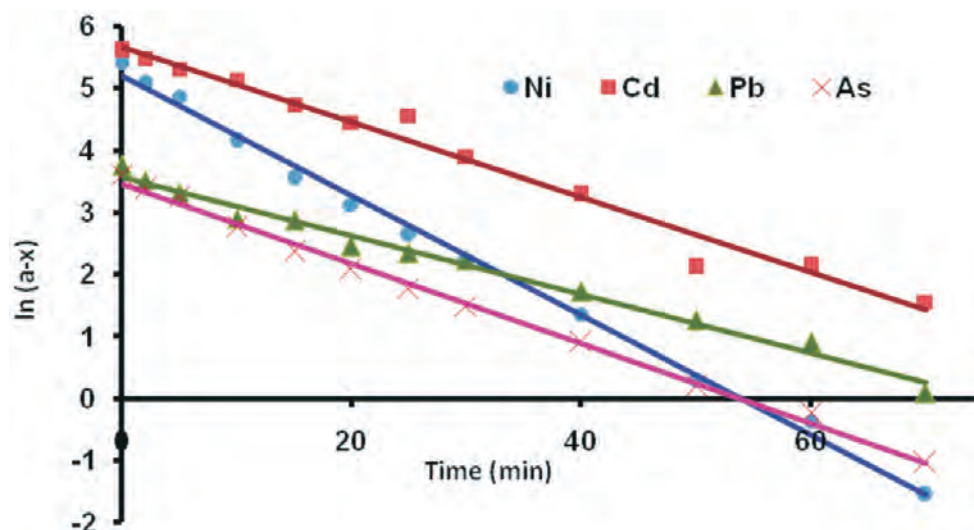


Figure 4 First-order kinetics of adsorption of As, Cd, Ni and Pb on electrospun nylon-6-AMMP nanofibre sorbent.

Table 2 Rate constants and the correlation coefficients for first-order adsorption of metals on electrospun nylon-6-AMMP nanofibre sorbent

| Metal | k/min^{-1} | r^2 |
|-------|---------------------|--------|
| Cd | 0.0604 | 0.9781 |
| Ni | 0.0963 | 0.9961 |
| Pb | 0.0474 | 0.9873 |
| As | 0.0642 | 0.9961 |

trations of a solute on the surface of a sorbent to the concentration of the solute in the liquid with which it is in contact as:

$$\frac{x}{m} = kC^{\frac{1}{n}}, \quad (2)$$

where x is the mass of solute adsorbed on a fixed mass m of sorbent, C is the equilibrium concentration of the solution, and k and n are constants.

The log of equation 2 gives:

$$\log\left(\frac{x}{m}\right) = \log k + \frac{1}{n}C. \quad (3)$$

It could be deduced from Equation 3 that a plot of $\log(x/m)$ vs $\log C$ should be a straight line if the adsorptions of heavy metals

on the electrospun nylon-6 sorbents followed the Freundlich model. Figure 5 shows the isotherms obtained for the individual metals.

The Freundlich isotherm best fits a wide range of experimental data because it is based on empirical results and not on theoretical assumptions.⁴³ The benefit of the isotherm is that it could be used to calculate the equilibrium concentration. In any case, adsorptions on the nanofibres sorbent were not expected to obey the Langmuir model due to non-uniformity of the sorbent's surface.

3.8. Method Validation

Table 3 gives the quality control parameters regarding the determination of metal concentrations in aqueous solutions. Accuracy of the determinations, expressed as relative error between the certified and the observed values of the reference material were $\leq 0.2\%$ for all the metals. The precision of these measurements expressed as relative standard deviation on five independent determinations, was also satisfactory, being lower than 3% in all cases.⁴⁴ The LOD of the metals ranged from $3.0 \pm 0.01 \mu\text{g L}^{-1}$ for Cd to $10.5 \pm 0.2 \mu\text{g L}^{-1}$ for As. The LOQ was $\leq 45 \mu\text{g L}^{-1}$ for all metals.

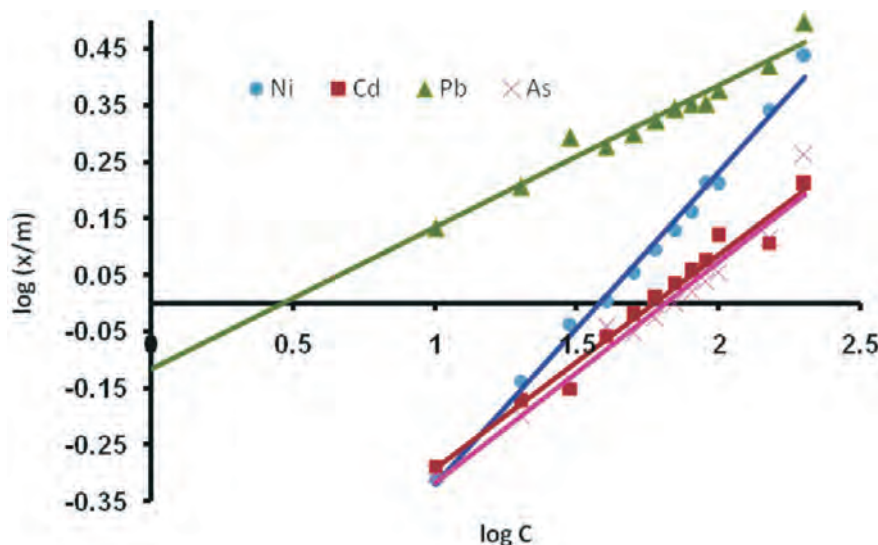


Figure 5 Freundlich isotherm depicting the adsorption of As, Cd, Ni and Pb on electrospun nylon-6-AMMP nanofibre sorbent.

Table 3 Analytical quality control parameters determined using the SEP-3 and BCR[®]-certified referenced groundwater.

| | SEP-3 | | | BCR [®] 610 | | | LOD/ $\mu\text{g L}^{-1}$ | | LOQ/ $\mu\text{g L}^{-1}$ | |
|----|--|--------------------------------------|------------------|-------------------------------|--|--------------------------------------|---------------------------|-------------------------------|---------------------------|------------------------|
| | Certified concentration/ $\mu\text{g L}$ | Concentration found/ $\mu\text{g L}$ | Relative error % | Relative standard deviation % | Certified concentration/ $\mu\text{g L}$ | Concentration found/ $\mu\text{g L}$ | Relative error % | Relative standard deviation % | | |
| As | – | – | – | – | 10.8 (0.4) | 10.5 | +0.3 | 2.8 | 10.5 (0.20) | 33 (0.91) |
| Cd | 50.2 (0.000) | 50.1 (0.006) | –0.10 | 0.20 | 2.94 (0.08) | 3.00 | +0.06 | 2.04 | 3.0 (0.01) | 13.3 (0.01) |
| Ni | 898.0 (7) | 899.6 (0.005) | +1.60 | 0.18 | – | – | – | – | 18 [§] (0.09) | 45 [§] (0.02) |
| Pb | 1498.0 (9) | 1496.0 (2) | –2.0 | 0.13 | 7.78 (0.13) | 7.82 | +0.04 | 0.51 | 6.5 (0.001) | 14.5 (0.04) |

*Standard deviations in brackets.

§Value is based on the SEP-3 concentration.

Table 4 Summary of pre-concentration achieved by the three methods.

| | River | | | Tap | | | Sea | | | Treated wastewater | | | Untreated wastewater | | |
|----|-------|-------|-------|-------|-------|------|-------|-------|-------|--------------------|-------|-------|----------------------|-------|-------|
| | X | D | F | X | D | F | X | D | F | X | D | F | X | D | F |
| As | 0.23 | 0.73 | 0.34 | 0.80 | 0.76 | 0.67 | 0.40 | 0.59 | 0.54 | 0.67 | 0.17 | 0.03 | 0.88 | 0.88 | 0.82 |
| Cd | 0.00 | 0.15 | 0.10 | 0.01 | 0.15 | 0.13 | 0.19 | 0.11 | 0.00 | 0.20 | 1.88 | 1.80 | 3.48 | 2.31 | 1.36 |
| Ni | 6.30 | 6.69 | 6.55 | 9.43 | 10.88 | 9.60 | 11.65 | 11.51 | 10.31 | 39.34 | 48.99 | 41.99 | 25.73 | 25.25 | 23.77 |
| Pb | 21.90 | 22.11 | 21.09 | 11.27 | 11.66 | 9.87 | 10.45 | 9.80 | 10.49 | 18.86 | 19.63 | 12.41 | 24.26 | 20.02 | 18.14 |

X = digested HNO₃+H₂O₂; D = digested with aqua regia; F = adsorbed using electrospun nanofibres

3.9. Comparison with Digestion Protocols

Using the metal concentrations obtained from samples that were only spiked with HNO₃ as the bench mark, the capacity of the sorbent to pre-concentrate metals (As, Cd, Ni and Pb) was compared with those of standard digestion protocols, namely aqua regia and HNO₃+H₂O₂ digestions. Pre-concentration factors achieved for each method, relative to spiking, were computed using (4)

$$\text{in Pre-concentration} = \frac{[\text{method}]}{[\text{spiking}]} \times 100. \quad (4)$$

The pre-concentration factors achieved by the three methods are summarized in Table 4. The concentrations of As (values) and Cd (values) in all the water samples were generally lower compared to those of Ni (values) and Pb (values). The three methods recorded similar levels of pre-concentrating Ni in river water samples; 6.30 for HNO₃+H₂O₂ digestion, 6.69 for aqua regia digestion and 6.55 for adsorptions. The observed similar levels of pre-concentrating Ni in river water samples suggest that any of the three methods could be used for enriching Ni in river water samples. Pb ions in the river water samples were pre-concentrated slightly better using the two digestion methods (pre-concentration factor ~22) compared to adsorptions (pre-concentration factor ~21). With regards to As and Cd in river water samples, the efficiency of pre-concentration followed the trend: aqua regia digestion > adsorption > HNO₃+H₂O₂ digestion.

The efficiencies of pre-concentrating As in tap and sea water samples were almost the same for all the three methods. Aqua regia digestion offered the best pre-concentration procedure for Cd and Ni followed by the adsorption method. The digestion methods recorded higher pre-concentration efficiencies (11.66 for aqua regia digestion and 11.27 for HNO₃+H₂O₂ digestion) compared to the adsorption method (9.87). The sorbent could not pre-concentrate Cd in sea water although the concentrations detected using the digestion methods were higher than the LOD of the adsorption method. This could be due to matrix effect of the sea water. The HNO₃+H₂O₂ and aqua regia digestion methods recorded pre-concentration factors of 0.19 and 0.11, respectively, for Cd in sea water samples. The order of pre-concentration efficiencies for Ni in sea water was HNO₃+H₂O₂ digestion > aqua regia digestion > adsorption. With respect to uptake of Pb in sea water, the sorbent performed better (factor ~10.49) than both HNO₃+H₂O₂ (10.45) and aqua regia (9.80).

In the treated wastewater samples, the aqua regia digestion method achieved higher pre-concentration levels than the other two methods. The adsorption process was also slightly more efficient than the HNO₃+H₂O₂ digestion with respect to Cd and Ni. However, the efficiency of HNO₃+H₂O₂ digestion superseded that of the adsorption process in terms of Ni and Pb in the treated water samples. The pre-concentration efficiencies of the two acid digestion protocols in untreated wastewater samples were slightly higher than that of the adsorption process, for all the metals investigated. Ideally, one expects fouling on the sorbent when it is applied in complex matrices like untreated wastewater. The high performance of the nanofibre sorbent, relative to other membrane sorbents, is attributable to the highly porous nature of the nanofibres.

3.10. Reusability of Nanofibre Sorbent

The sorbent showed a remarkable stability in reusability. Sorbent reusability, which used to be a challenge with some of the electrospun nanofibre sorbents, we prepared earlier was not

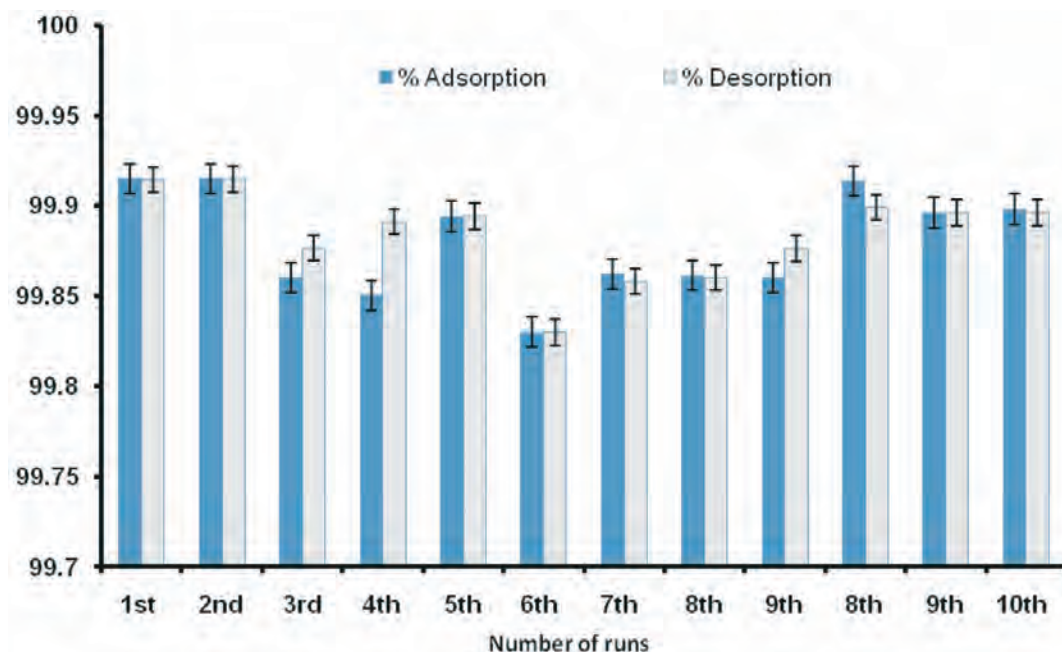


Figure 6 Reusability of the sorbent.

encountered in this work. This is because the ligand was covalently bonded to a mechanically stable nylon-6 backbone. Leaching of the ligand and loss of traces of the sorbent during use was, therefore, restricted. About 0.1 reduction in adsorption/desorption efficiencies was observed at the 10th round of usage (Fig. 6).

4. Conclusion

Nylon-6 was successfully functionalized with a Schiff base ligand that has a high affinity for toxic metal ions. The functionalized polymer was electrospun to obtain nanofibres which were then stamped out into sorbents for uptake of toxic metal ions from different aqueous environments. The sorbent tuned as function of pH, for both uptake and release of the metals. The sorbent exhibited high pre-concentration capacities that were comparable to acid digestion protocols currently in use. It also presents the advantage of good reusability and high chemical stability. Electrospun functionalized nylon-6 nanofibre sorbent was successfully applied to pre-concentrate toxic metals from different aqueous environments.

Acknowledgements

NRE, SEANAC, WRC, Sasol and Rhodes University are acknowledged for financial support.

References

- N.R. Axtell, S.P.K. Sternberg and K. Claussen, *Bioresour. Technol.*, 2003, **89**, 41
- O. Akoto, T.N. Bruce and G. Darko, *Environ. Monit. Assess.*, 2010, **161**, 413–422.
- M. Jamshidi, M. Ghaedi, K. Mortazavi, M. Biareh and M. Soylak, *Food Chem. Toxicol.*, 2011, **49**, 1229–1234.
- Y. Zhang, R. Qu, C. Sun, H. Chen, C. Wang, C. Ji, P. Yin, Y. Sun, H. Zhang and Y. Niu, *J. Hazard. Mater.*, 2009, **163**, 127–135.
- A.N. Vasiliev, L.V. Golovko, V.V. Trachevsky, G.S. Hall and J.G. Khinast, *Micropor. Mesopor. Mater.*, 2009, **118**, 251–257.
- J. Aguado, J.M. Arsuaga, A. Arencibia, M. Lindo and V. Gascón, *J. Hazard. Mater.*, 2009, **163**, 213–221.
- A. Heidari, H. Younesi and Z. Mehraban, *Chem. Eng. J.*, 2009, **153**, 70–79.
- P.C. Mishra and R.K. Patel, *J. Hazard. Mater.*, 2009, **168**, 319–325.
- M. Ezoddin, F. Shemirani, K.H. Abdi, M.K. Saghezchi and M.R. Jamali, *J. Hazard. Mater.*, 2010, **178**, 900–905.
- A. Gundogdu, D. Ozdes, C. Duran, V.N. Bulut, M. Soylak and H.B. Senturk, *Chem. Eng. J.*, 2009, **153**, 62–69.
- A.M.B. Hamissa, A. Lodi, M. Seffen, E. Finocchio, R. Botter and A. Converti, *Chem. Eng. J.*, 2010, **159**, 67–74.
- M. Mapolelo, N. Torto and B. Prior, *Talanta*, 2005, **65**, 930–937.
- P. Miretzky, C. Muñoz and A. Carrillo-Chavez, *Bioresource. Technol.*, 2010, **101**, 2637–2642.
- A. Sari and M. Tuzen, *J. Hazard. Mater.*, 2009, **164**, 1004–1011.
- Q. Tang, X. Tang, M. Hu, Z. Li, Y. Chen and P. Lou, *J. Hazard. Mater.*, 2010, **179**, 95–103.
- S. Oh, M.Y. Kwak and W.S. Shin, *Chem. Eng. J.*, 2009, **152**, 376–388.
- B. Rezaei, E. Sadeghi and S. Meghdadi, *J. Hazard. Mater.*, 2009, **168**, 787–792.
- W.E. Teo, M. Kotaki, X.M. Mo and S. Ramakrishna, *Nanotechnology*, 2005, **16**, 918–924.
- N. Daels, S.D. Vrieze, B. Decostere, P. Dejjans, A. Dumoulin, K.D. Clerck, P. Westbroek and S.W.H.V. Hulle, *Desalination*, 2010, **257**, 170–176.
- S. Sakai, K. Antoku, T. Yamaguchi and K. Kawakami, *J. Membr. Sci.*, 2008, **325**, 454–459.
- Y. Wang and Y.L. Hsieh, *J. Membr. Sci.*, 2008, **309**, 73–81.
- L. Wu, X. Yuan and J. Sheng, *J. Membr. Sci.*, 2005, **250**, 167–173.
- D. Adeyemi, J. Mokgadi, J. Darkwa, C. Anyakora, G. Ukpo, C. Turner and N. Torto, *Chromatographia*, 2011, **73**, 1015–1020.
- S. Chigome, G. Darko, U. Buttner and N. Torto, *Anal. Methods*, 2010, **2**, 623–626.
- G. Darko, S. Chigome, Z. Tshentu and N. Torto, *Analytical Letters*, 2011, **44**, 1855–1867.
- M. Ziabari, V. Mottaghitalab and A.K. Haghi, *Brazilian J. Chem. Eng.*, 2009, **26**, 53–62.
- US-EPA, EPA-821-R-01-010, Method 200.7, New York, 2001.
- J. Sastre, A. Sahuquillo, M. Vidal and G. Rauret, *Anal. Chim. Acta.*, 2002, **462**, 59–72.
- C.M. Sun, R.J. Qu, C.N. Ji, C.H. Wang, Y.Z. Sun, Z.W. Yue, G.X. Chang, *Talanta*, 2006, **70**, 14–16.
- SUN B (1994). *Chin J PolymSci* **12**(1): 57–65.
- J. Greener, B. Abbasi and E. Kumacheva, *Lab Chip.*, 2010, **10**, 1561–1566.

- 32 D. Hussain, F. Loyal, A. Greiner and J.H. Wendorff, *Polymer*, 2010, **51**, 3989–3997.
- 33 S. DeVrieze, B. DeSchoenmaker, Ö. Ceylan, J. Depuydt, L.V. Landuyt, H. Rahier, G.V. Guy Van Assche and K. DeClerck, *J. Appl. Polym. Sci.*, 2011, **119**, 2984–2990.
- 34 G.-Y. Oh, Y.-W. Ju, M.-Y. Kim, H.-R. Jung, H.J. Kim and W.-J. Lee, *Sci. Total. Environ.*, 2008, **393**, 341–347.
- 35 W.G. Shim, C. Kim, J.W. Lee, J.J. Yun, Y. Jeong, H. Moon and K.S. Yang, *J. Appl. Polym. Sci.*, 2006, **102**, 2454–2462.
- 36 Y.J. Ryu, H.Y. Kim, K.H. Lee, H.C. Park and D.R. Lee, *Europe. Polym. J.*, 2003, **39**, 1883–1889.
- 37 W. Stumm, *Chemistry of the Solid–Water Interface*. John Wiley and Sons, New York, 1992.
- 38 X. Guo, Y. Du, F. Chen, H.S. Park and Y. Xie, *J. Colloid. Interf. Sci.*, 2007, **314**, 427–433.
- 39 W. S. Wan Ngah, A. Kamari, S. Fatinathan and P. W. Ng, *Adsorption*, 2006, **12**, 249–257.
- 40 Y. Ren, X. Wei, M. Zhang, *J. Hazard. Mater.*, **158**, 14–22.
- 41 L. Zhou, Y. Wang, Z. Liu and Q. Huang, *J. Hazard. Mater.*, 2009, **161**, 995–1002.
- 42 M.L. Pierce and C.B. Moore, *Water. Res.*, 1982, **16**, 1247–1253.
- 43 S. Sohn and D. Kim, *Chemosphere*, 2005, **58**, 115–123.
- 44 W. Huber, *Accred. Qual. Assur.*, 2003, **7**, 256–257.